Deposition rate of supersaturated silicic acid on Na-type bentonite as a backfilled material in the geological disposal

著者	Tsuyoshi Sasagawa, Taiji Chida, Yuichi Niibori
journal or publication title	Applied Geochemistry
volume	98
page range	377-382
year	2018-08-24
URL	http://hdl.handle.net/10097/00128831

doi: 10.1016/j.apgeochem.2018.08.007

Deposition rate of supersaturated silicic acid on Na-type bentonite as a backfilled material in the geological disposal

Tsuyoshi Sasagawa[1], Taiji Chida[1], Yuichi Niibori[1]

1. Department of Quantum Science and Energy Engineering, Graduate School of Engineering, Tohoku University, Sendai 9808579, Japan

Abstract

When constructing geological disposal systems for radioactive waste, saline groundwater, originating from fractured rock matrices surrounding disposal tunnels, may reduce bentonite swelling properties and accelerate radionuclide migration. In contrast, high alkaline groundwater, caused by the use of cementitious materials, induces supersaturated conditions with regard to silicic acid. The resulting deposition of silicic acid may decrease the hydraulic conductivity of flow paths. Therefore, this study experimentally examined the apparent deposition rate constant, *k* (m/s), by considering the supersaturated concentration of silicic acid and deep-underground temperatures (288–323 K). As a result, the apparent deposition rate constants, obtained experimentally, were not affected by an initial supersaturated concentration and were only slightly affected by

temperature. We estimated the apparent activation energy at 8.9 kJ/mol. Furthermore, because the Damköhler number, described by the ratio between the apparent deposition rate constant and the groundwater flow rate, had a large value, exceeding 10^3, the deposition of supersaturated silicic acid may cause the narrowing flow paths. These results suggest that silicic acid deposition contributes to retardation effects via the decrease of the hydraulic conductivity in backfilled tunnels.

Keywords: deposition rate, supersaturated silicic acid, Na-type bentonite, backfilling material, geological disposal

1. *INTRODUCTION*

1.1. *Utilization of bentonite as a backfill material*

In Japan, high-level radioactive wastes and trans-uranic wastes (TRU waste), which are comprised of long half-life radionuclides, are disposed of deep underground at depths of 300 m or more [1,2]. Generally, throughout Japan, deep-underground environments are completely saturated with abundant groundwater. Therefore, any newly constructed radioactive waste repositories will become saturated again after backfilling. In such a geological environment, Na-type bentonite, which is characterized by high

swelling properties, will be used to fabricate the backfill materials placed in repository tunnels in order to restrict groundwater flow. However, as shown in Figure 1, after backfilling, extra flow paths may form via significant groundwater infiltration and/or high saline conditions [1]. In particular, saline groundwater increases the hydraulic conductivity of Na-type bentonite by decreasing its swelling properties [3,4]. Under such conditions, groundwater flow through bentonite flow paths facilitates the migration of radionuclides in the backfilled tunnels.

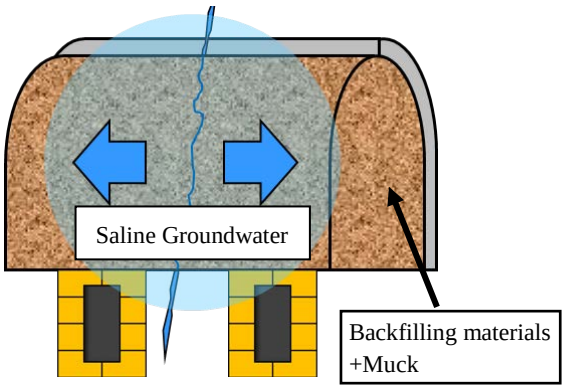

Figure 1: Flow-path formation in backfilled tunnels. Here, the flow-path means a region where groundwater easily passes locally (not just a single crack).

1.2. *Redistribution of silicic acid in the repository*

Silicic acid, which is found in most minerals, is a key factor for estimating the degree and magnitude of alteration in a disposal environment. As is commonly known, silicic acid chemical species are significantly influenced by changes in pH. In the disposal system, the large amount of cementitious materials, used for the construction of the disposal facilities, causes significant pH changes in and around the repository.

Groundwater pH varies between 8 and 13, via leaching of alkaline components such as sodium, potassium, and calcium from cementitious materials [5,6]. This high alkaline groundwater dissolves clay minerals and numerous silicate materials, thus increasing hydraulic conductivity in and around the repository, which releases silicic acid into groundwater. Because this groundwater contains high concentrations of silicic acid and mixes with natural groundwater downstream, the natural groundwater pH decreases to 8. Concurrently, owing to a significant decrease in silicic acid solubility, supersaturated silicic acid predominantly deposits onto solid phases, partly forming colloidal silicic acid in a liquid phase. In this study, we used the word “deposition” rather than “precipitation”. Deposition is a phenomenon in which a molecule is bonded to the solid surface, and precipitation is a phenomenon in which molecules are bonded together to form precipitating colloids. This redistribution behavior of silicic acid may restrict the migration of groundwater and radionuclides because of the decrease in the hydraulic conductivity of flow paths with the deposition of supersaturated silicic acid. Some studies have examined this redistribution effect via laboratory experiments, assuming that fractures in the host rock act as a solid phase [7–11]. In addition, several natural-analog surveys indicate that silicic acid redistribution causes clogging of the flow paths [12,13]. However, these previous studies have mainly focused on crystalline rocks (e.g., granite

from Japan) and have used the comprising minerals as the solid phase for silicic acid deposition around the repository.

1.3. *Objectives of the study*

The objectives of this study are to estimate the supersaturated silicic acid deposition rate of Na-type bentonite and to assess the contribution of such deposition to the decrease in the hydraulic conductivity of flow paths. As described in Section 1.2, several studies have detected flow-path narrowing and clogging via silicic acid deposition, under some conditions, but there are very few studies that have targeted clay minerals such as bentonite. In a recent study, we examined the dynamic behavior between silicic acid and a Ca-type bentonite. The results from this study suggest that flow paths in backfilled material will be narrowed by silicic acid deposition onto Ca-type bentonite [11]. However, because Na-type bentonite is the main backfill material component, it is necessary to investigate experimentally silicic acid deposition behavior onto Na-type bentonite. In addition, previous studies have reported that silicic acid polymerization depends significantly on changes in temperature [14]. The underground temperature is estimated to be 318 K at a depth of 1000 m in the geological repository, with a temperature gradient of 3 K/100 m [1]. Therefore, to demonstrate narrowing flow paths in backfilled

tunnels with silicic acid redistribution, this study examined the effects of temperature on the deposition behavior of supersaturated silicic acid on Na-type bentonite under saline conditions. Especially, we focused on estimating the apparent deposition rate constants based on experimental results to assess the narrowing effect of flow paths via with silicic acid deposition.

2. *EXPERIMENTAL*

2.1. *Bentonite sample*

Kunigel V1 powder (Na-type bentonite, purchased from Kunimine Industries Co., Ltd.) was used as the solid phase. The mineral composition of Kunigel V1 is shown in Table I [15]. Na-type bentonite is frequently used as a backfill or buffer material in geological repository construction, because it has low hydraulic conductivity with high swelling and absorptivity properties for radionuclides due to its layer structure. The surface area of Na-type bentonite was estimated to be 19.17 m^2/g with the Brunauer, Emmett, and Teller (BET) method and 385.4 m^2/g with the ethylene glycol monoethyl ether (EGME) method [16]. In general, the EGME method value exceeds the BET method value. This is because the EGME method estimates the specific surface area, including the interlayer, whereas the BET method estimates the whole specific surface area except

for the montmorillonite interlayer. The specific surface area is an important factor when estimating apparent deposition rate constants (described later). However, it is unclear whether silicic acid is deposited on the montmorillonite interlayer structure. Therefore, both specific surface area values were used for estimating the apparent deposition rate constant, k (m/s).

Table I. The mineral composition of Kunigel V1(Na-type bentonite) [15]

Smectite	46–49	Calcite	2.1–2.6
Quartz	0.5–0.7	Dolomite	2.0–2.8
Chalcedony	37–38	Analcime	3.0–3.5
Plagioclase	2.7–5.5	Pyrite	0.5–0.7

2.2. *Experimental method and conditions*

Deposition experiments were performed using a batch-type method under a nitrogen atmosphere. Details about the experimental methods used in this study can be found in Sasagawa et al. [10]. The supersaturated silicic acid concentration was determined using the solubility of amorphous silica, which we assumed as the deposition material at each temperature. The solubility temperature dependence was the concentration of soluble silicic acid that reached equilibrium at 6 h after the start of the experiment. Previous studies on the solubility temperature dependence of silicic acid, at high ionic strength, provided insufficient data. The equilibrium concentration of silicic

acid was set to 2.18 mmol/dm^3 at 288 K, 2.38 mmol/dm^3 at 298 K, and 3.55 mmol/dm^3 at 323 K. For example, we adjusted the total silicic acid concentration to 10.38 mmol/dm^3 to set the supersaturated concentration to 8 mmol/dm^3 at 298 K. Since silicic acid concentration in groundwater is largely affected by pH, temperature, specific surface area, mineral species, dissolved ions, flow rate and so on, the concentration cannot be determined simply. Therefore, in this study, the initial supersaturated concentration of silicic acid is given as a parameter of the experiments, and the apparent deposition rate constants were arranged so as not to depend on the initial supersaturated concentration. First, the silicic acid solution diluting water glass (Na_2SiO_3 solution), at the determined concentration, was poured into a polyethylene vessel. Then, solid-phase Na-type bentonite was poured into the silicic acid solution (pH > 10). Subsequently, nitric acid and a buffer solution (a mixture of 2-morpholinoethanesulfonic acid monohydrate and tris(hydroxymethyl)aminomethane) were added to the solution to adjust the pH to 8. At this point, we initiated silicic acid deposition onto the Na-type bentonite. During the 360 min deposition experiments, we sampled aliquots at given time intervals. The sample solution that measures the silicic acid concentration was separated from the solid phase using a 0.45 μm membrane filter. Table II displays the experimental conditions for this study. To confirm the effect coexisting the solid phase, we also performed both

polymerization and precipitation experiments without the Na-type bentonite. For estimating the deposition behavior under the conditions without co-precipitation, this present study did not add Ca ions, which will increase in concentration around the repository due to leaching from cementitious materials. In general, alkali species in cementitious materials, such as Na and K ions, are leached from the cement before Ca ions. In other words, the redistribution of silicic acid around the repository should be considered not only in Ca-rich but also in Ca-absent conditions [5, 6]. Of course, the influence of Ca ions on the redistribution of silicic acid is a critical issue for estimating the silicic acid deposition in the long run. Our future study will focus on the deposition behavior of silicic acid under Ca-rich conditions. In addition, since the dissolution rate of the silicate minerals in this experimental condition is sufficiently small, it was assumed that there is little elution of silicic acid from silicate minerals.

Table II. Experimental conditions.

	Supersaturated concentration effects (Figures 2 and 3)	Temperature effects (Figure 6)	Without solid phase (Figure 4)
Initial supersaturated concentration of silicic acid	1, 2, 4, 6, 8, 10 mmol/dm^3	2, 8 mmol/dm^3	8 mmol/dm^3
Temperature	298 K	288, 298, 323 K	298 K
Amount of solid phase	2.5, 5.0, 7.5 g	2.5, 5.0, 7.5 g	0 g
Total volume of liquid phase	250 mL	250 mL	250 mL
pH	8	8	8
NaCl concentration	0.6 mol/dm^3	0.6 mol/dm^3	0, 0.6 mol/dm^3
Stirring rate	300 rpm	300 rpm	300 rpm
Filter diameter	0.45 μm	0.45 μm	0.45 μm

2.3. *Silicic acid quantification*

This study has defined the state of silicic acid for the deposition experiments as well as soluble silicic acid, colloidal silicic acid, and their deposition on Na-type bentonite. Soluble silicic acid has low-polymerization molecules (monomeric and oligomeric [17]), whose concentrations were quantified by the silicomolybdenum-yellow method [18]. The total concentrations, including both soluble and colloidal silicic acid in the liquid phase, were measured by inductively coupled plasma-atomic emission spectroscopy. Therefore, colloidal silicic acid was calculated as the difference between the liquid phase total and the soluble silicic acid. We calculated silicic acid deposition onto Na-type bentonite by subtracting the liquid phase total from the initial total silicic acid concentration. Note that we accounted for colloidal silicic acid deposition, which was removed from the liquid

phase by a 0.45 μm membrane filter.

3. *RESULTS AND DISCUSSION*

3.1. *Effects of supersaturated silicic acid concentrations*

Figures 2 and 3 show the deposition experiment results for initial supersaturated concentrations of 2 and 8 mmol/dm^3 and 2.5, 5.0, and 7.5 g of Na-type bentonite. The vertical axis, *f*, is the fraction of soluble silicic acid, colloidal silicic acid, and deposition on the Na-type bentonite to the initial supersaturated silicic acid concentration. The following equation describes the fraction of soluble silicic acid:

$$f_s = \frac{c_s - c_e}{c_{ini} - c_e} \quad . (1)$$

Equations (2) and (3) describe the fractions of colloidal silicic acid and deposition, respectively:

$$f_c = \frac{c_c}{c_{ini} - c_e} , (2)$$

$$f_d = \frac{c_d}{c_{ini} - c_e} , (3)$$

where c_s is the soluble silicic acid concentration (in mol/dm^3), c_e is amorphous silica solubility (in mol/dm^3), c_{ini} is the initial silicic acid concentration (in mol/dm^3), c_c is the colloidal silicic acid concentration (in mol/dm^3), and c_d is silicic acid deposition (in mol/dm^3). As shown in Figures 2 and 3, silicic acid deposition on Na-type bentonite and the formation of colloidal silicic acid progressed, and soluble silicic acid decreased. The experimental results, under different conditions, show similar tendencies. In particular, large amounts of colloidal silicic acid formed under conditions with higher supersaturated concentrations and smaller amounts of the solid phase. In this case, not only does soluble silicic acid deposit on the solid phase, it also promotes the precipitation of colloidal silicic acid when associated with coexisting electrolytes such as NaCl. To confirm colloidal silicic acid precipitation behavior, we performed polymerization experiments, without the solid phase, as shown in Figure 4. In Figure 4(a), colloidal silicic acid increased proportionally to decreasing soluble silicic acid, and the precipitation of silicic acid was not observed. In Figure 4(b) for 0.6 mol/dm^3 NaCl, precipitation increased significantly after 240 min, along with an increase in colloidal silicic acid formation, which became faster than the results shown in Figure 4(a) until 180 min. These results suggest that Na ions accelerate silicic acid polymerization due to compression of the electric double layer

[19]. Then, colloidal silicic acid precipitated or was separated by a 0.45 μm membrane filter from the solution due to large colloid particle formation. However, such precipitation behavior requires a significant period of time after colloidal silicic acid formation, as shown in Figure 4(b). Therefore, the deposition behavior, such as that observed in Figures 2 and 3, does not cause colloidal silicic acid precipitation but rather it is caused by the deposition of soluble silicic acid onto Na-type bentonite. Furthermore, the proportion of the solid-phase surface area to the volume of the liquid phase is generally large in backfilled tunnels. Considering that deposition increases with increasing amounts of Na-type bentonite, as shown in Figures 2 and 3, we predict that soluble silicic acid deposition will be more predominant than colloidal silicic acid formation.

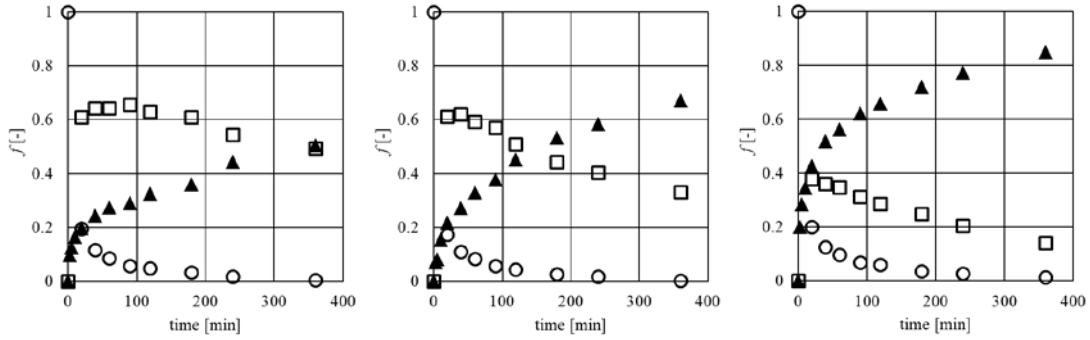

(a) (b) (c)

Figure 2: Silicic acid deposition for an initial supersaturated concentration of 8 mmol/dm^3 and solid-phase amounts of (a) 2.5 g, (b) 5.0 g, and (c) 7.5 g. (▲ denotes deposition, ○ denotes soluble silicic acid, and □ denotes colloidal silicic acid.)

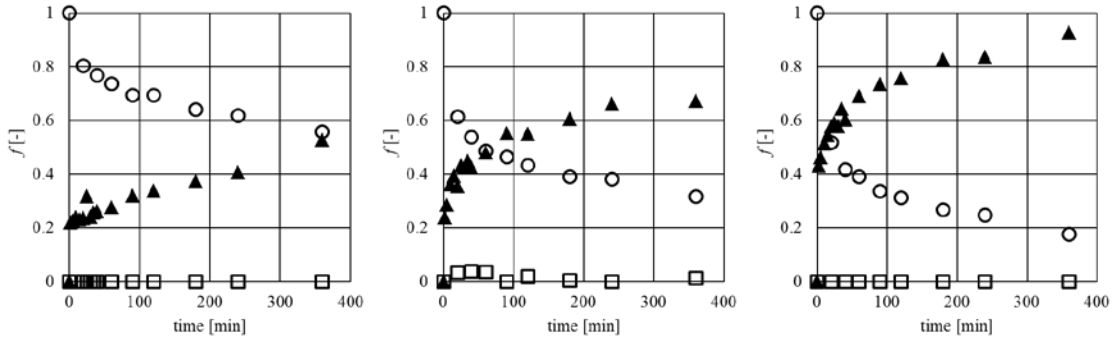

(a) (b) (c)

Figure 3: Silicic acid deposition for a supersaturated concentration of 2 mmol/dm^3 and solid-phase amounts of (a) 2.5 g, (b) 5.0 g, and (c) 7.5 g. (▲ denotes deposition, ○ denotes soluble silicic acid, and □ denotes colloidal silicic acid.)

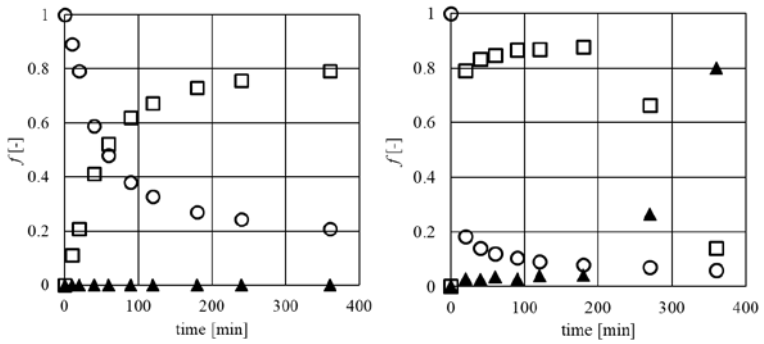

(a) (b)

Figure 4: Silicic acid polymerization behavior without the solid phase for a supersaturated concentration of 8 mmol/dm^3. (NaCl concentrations of (a) 0 M and (b) 0.6 M. ▲ denotes precipitation, ○ denotes soluble silicic acid, and □ denotes colloidal silicic acid.)

3.2. *Apparent deposition rate constants*

The apparent deposition rate constants, k (m/s), were calculated from the following equations using the initial deposition rate, r_{ini}, from the experimental results. First, equation (4) describes the deposition of silicic acid as follows:

$$c_d = (c_{ini} - c_e) - c_c - (c_s - c_e) = c_{ini} - c_s - c_c \quad . (4)$$

Then, equation (5) describes the change of c_d per unit time as follows:

$$\frac{dc_{\mathrm{d}}}{dt} = -\frac{d\left(c_{\mathrm{s}} - c_{\mathrm{e}}\right)}{dt} - \frac{dc_{\mathrm{c}}}{dt}, \quad (5)$$

where t is time (s). In addition, equations (6) and (7) describe changes in soluble silicic acid and colloidal silicic acid per unit time as follows:

$$-\frac{d}{dt}\left(c_{\mathrm{s}} - c_{\mathrm{e}}\right) = kA\left(c_{\mathrm{s}} - c_{\mathrm{e}}\right) + k_{c}^{+}\left(c_{\mathrm{s}} - c_{\mathrm{e}}\right)^{n} - k_{\mathrm{c}}^{-}c_{\mathrm{c}}^{m}, \quad (6)$$

$$\frac{dc_{\mathrm{c}}}{dt} = k_{\mathrm{c}}^{+}\left(c_{\mathrm{s}} - c_{\mathrm{e}}\right)^{n} - k_{\mathrm{c}}^{-}c_{\mathrm{c}}^{m}, \quad (7)$$

where amorphous silica solubility, c_{e}, is constant with time.

In equations (6) and (7), k is the apparent deposition rate constant (m/s), A is the specific surface area per unit volume, calculated via the solid–liquid ratio (1/m), k_{c}^{+} is the polymerization rate constant, k_{c}^{-} is the depolymerization rate constant, and n and m are reaction orders. The parameter A can also be described by $A = am/V$, where a is the specific surface area (m^2/g). Therefore, by combining equations (5)–(7), we can describe the change in silicic acid deposition as follows:

$$\frac{dc_{\mathrm{d}}}{dt} = kA\left(c_{\mathrm{s}} - c_{\mathrm{e}}\right) \quad . \quad (8)$$

Here, by dividing both sides of equation (8) by the initial supersaturated concentration ($c_{ini}-c_e$), and by substituting $f_s = 1$ at $t = 0$, we obtain equation (9):

$$\left.\frac{df_d}{dt}\right|_{ini} = r_{ini} = kA \quad . (9)$$

We calculated the apparent deposition rate constant, k (m/s), based on the deposition rate, r_{ini}, which was estimated by fitting equation (9) to the experimental data results from 0 to 40 min. At the initial condition, the specific surface area, A, equals the value measured by both the BET and EGME specific surface area methods.

Figure 5 shows the relationship between the r_{ini} values, obtained from the experimental results, and the solid-phase surface area. The slope in Figure 5 is equivalent to the apparent deposition rate constant, k (m/s). In Figure 5, because the slope contribution ratio, R^2, is nearly 1, the deposition rates are linearly proportional to the surface area for ratios of supersaturated concentrations to surface areas.

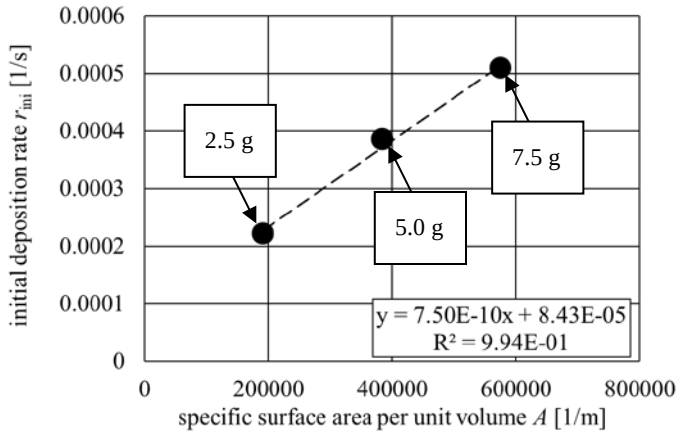

Figure 5: Apparent deposition rate constant calculations (initial supersaturated concentration: 2 mmol/dm^3; temperature: 298 K; specific surface area: 19.17 m^2/g).

Table III summarizes the apparent deposition rate constants, *k* (m/s), calculated from the experimental results. As shown in Table III, the apparent deposition rate constants were approximately constant during supersaturated concentration conditions because the fraction of deposition magnitude was normalized by the initial supersaturated concentration, as described in Section 3.1 and 3.2. For the specific surface area, the apparent deposition rate constants, calculated with the specific surface area from the BET method, were approximately one order of magnitude larger than those using the EGME method. Compared with a previous study using amorphous silica as a solid phase [10], the apparent deposition rate constants were the same order of magnitude as the value using the BET method in this study. These results suggest that the montmorillonite

interlayer, measured by the EGME method, hardly contributes to supersaturated silicic acid deposition. In general, the montmorillonite interlayer has a permanent negative charge due to isomorphous substitution. Anions such as silicic acid can very rarely penetrate such an interlayer. Therefore, we used the specific surface area measured using the BET method to calculate the apparent deposition rate constants in this study, in an attempt to gain more reasonable values.

Table III. Apparent deposition rate constants, k (m/s).

		Initial supersaturated concentration of silicic acid					
		1 mmol/dm^3	2 mmol/dm^3	4 mmol/dm^3	6 mmol/dm^3	8 mmol/dm^3	10 mmol/dm^3
Specific surface area	385.4 m^2/g (EGME)	4.63×10^{-11}	3.73×10^{-11}	2.04×10^{-11}	3.04×10^{-11}	3.31×10^{-11}	2.62×10^{-11}
	19.17 m^2/g (BET)	9.31×10^{-10}	7.50×10^{-10}	4.10×10^{-10}	6.11×10^{-10}	6.66×10^{-10}	5.26×10^{-10}

3.3. *Temperature effects on the deposition of silicic acid*

Figure 6 displays the effects of temperature on silicic acid deposition. From the figure, the deposition rate increases as the temperature increases between 288 and 323 K. This suggests that high temperature conditions, common in the deep underground, accelerate flow-path narrowing during silicic acid deposition on Na-type bentonite in backfilled tunnels. Moreover, by using the Arrhenius equation ($k = A^*\exp(-E_a/RT)$, where A^* is the frequency factor, E_a is the apparent activation energy (kJ/mol), R is the gas constant (J/(K·mol)), and T is the absolute temperature (K)), the Arrhenius plot is shown

in Figure 7, where we estimate the apparent activation energy at 8.9 kJ/mol using the apparent deposition rate constants listed in Table IV. This apparent activation energy is lower than that for silicic acid polymerization (approximately 40 kJ/mol or more) [14]. Such low activation energy is generally associated with dynamic behavior that is limited by diffusion processes or plural reactions. In this study, the stirring rate for each batch test barely affected the experimental results. Therefore, the relatively low activation energy is possibly due to inhibited silicic acid adsorption to the solid phase via an increase in temperature [20].

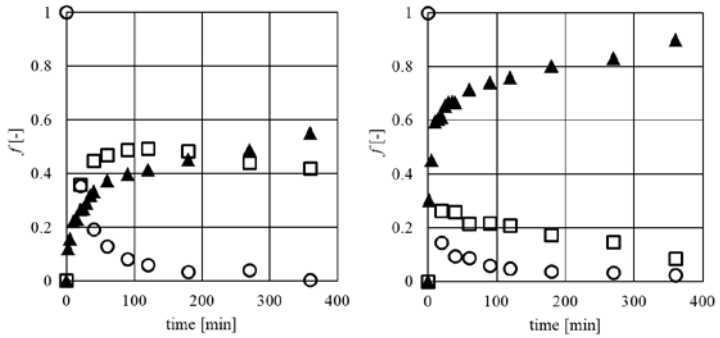

(a) (b)

Figure 6: Temperature effects on silicic acid deposition (initial supersaturated concentration: 8 mmol/dm^3; amount of solid phase: 5.0 g; temperature: (a) 288 K and (b) 323 K). (▲ denotes deposition, ○ denotes soluble silicic acid, and □ denotes colloidal silicic acid.)

Table IV. Apparent deposition rate constants, k (m/s) (temperature: 288, 298, and 323 K).

		Initial supersaturated concentration	
		2 mmol/dm^3	8 mmol/dm^3
Temperature	288 K	4.31×10^{-10} m/s	5.22×10^{-10} m/s
	298 K	7.50×10^{-10} m/s	6.66×10^{-10} m/s
	323 K	7.74×10^{-10} m/s	7.38×10^{-10} m/s

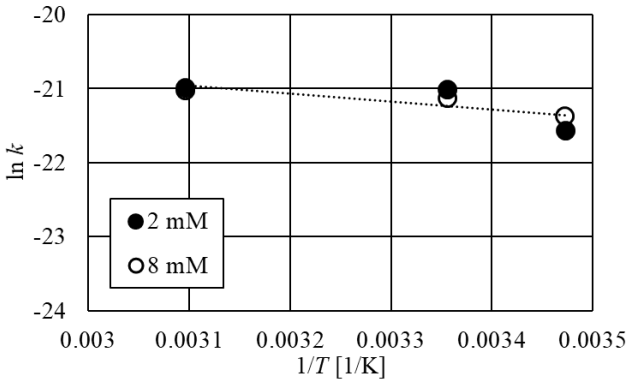

Figure 7: Arrhenius plot obtained from the experimental results listed in Table IV.

3.4. *Damköhler number*

To discuss the narrowing of flow paths with silicic acid deposition in backfilled tunnels from the viewpoint of comparing the deposition rate with groundwater flow, we discuss the apparent deposition rate constants in the context of the Damköhler number, which is a dimensionless number that represents the ratio of advection to chemical reaction [21]. The following equation describes the Damköhler number, D_a (–):

$$D_a = \frac{ka^* x}{u}, \quad (10)$$

$a^* = a\rho$,

where k is the apparent deposition rate constant (10^{-10} m/s, estimated in this study), a^* is the specific surface area per unit volume (1/m), x is the characteristic length (5 m, the tunnel diameter), u is the groundwater flow rate (50 m/year, the maximum flow rate for Japanese safety assessment (granite)), a is the specific surface area (19.17 m^2/g, estimated in this study), and ρ is the dry density (1.6 Mg/m^3). More details about the parameters x, u, and ρ can be found in the progress report [2]. These values were chosen conservatively so as not to overestimate the narrowing of flow paths. As a result, we calculated the Damköhler number values for silicic acid deposition onto Na-type bentonite as 10^3 or more. This indicates that silicic acid deposition reactions are much more predominant than groundwater advection in the flow paths of backfilled tunnels. Moreover, the previous study reported that 0.1 mm of fractures in the host rock will be narrowed to less than 10 % for approximately 200 years by mathematical simulations using the apparent deposition rate constants for the deposition of amorphous silica, which are similar to the values observed in this study [10]. Assuming that supersaturated silicic acid deposits on the solid surface of a porous medium as well as in host rock fractures, the hydraulic conductivity in tunnels backfilled by Na-type bentonite will also significantly decrease

with decreasing porosity [22]. Therefore, although flow paths form in backfilled tunnels associated with high saline conditions and significant groundwater infiltration, the supersaturated silicic acid deposition may narrow flow paths and reduce groundwater flow and retard radionuclide migration.

4. *CONCLUSIONS*

To understand the silicic acid deposition in backfilled tunnels, this study estimated the apparent deposition rate constants by performing deposition experiments using a Na-type bentonite. As a result, supersaturated silicic acid deposited on the Na-type bentonite increased significantly, and soluble silicic acid, in the liquid phase, decreased. Colloidal silicic acid also formed during experiments with elevated supersaturated concentrations and smaller solid-phase surface areas. We estimated the apparent deposition rate constants, based on the initial deposition rates, as 4.10–9.31 × 10^{-10} m/s at 298 K without dependencies on the initial supersaturated concentration, which ranged from 1 to 10 mmol/dm^3. For temperature effects between 288 and 323 K, the apparent deposition rate constants increased slightly with increasing temperature. We calculated the apparent activation energy as 8.9 kJ/mol, which was relatively small due to competition between dehydration reactions, associated with deposition, and silicic acid

adsorption. These results suggest that silicic acid deposition favors higher temperature conditions found in places such as deep, underground geological repositories. Furthermore, Damköhler number estimation shows that silicic acid deposition in backfilled tunnels is more predominant especially when compared with groundwater flow. Accordingly, these results indicate that the groundwater flow may be reduced and radionuclides retarded by the decrease in the hydraulic conductivity of flow paths associated with the supersaturated silicic acid deposition. Future studies should focus on hydraulic conductivity changes during silicic acid redistribution, which may be estimated via deposition experiments that monitor flow conditions using a flow reactor. The influence of Ca ions on silicic acid redistribution is also an important target. Furthermore, backfilled tunnel alteration over long time periods must be verified by mathematical analysis that considers advection, dispersion, and chemical reactions in the porous media.

Acknowledgments

JSPS KAKENHI, Grant-in-Aid for Scientific, supported this work (Research No. 18H01910, Grant-in-Aid for Scientific Research No. 17H01371, and Grant-in-Aid for JSPS Fellows No. 16J02619).

References

[1] JNC (Japan Nuclear Cycle development institute), 1999. *H12 Project to Establish the Scientific and Technical Basis for HLW Disposal in Japan, Supporting Report II, Repository Design and Engineering Technology.* JNC, Japan, JNC TN1400 99-021.

[2] Japan Nuclear Cycle Development Organization Institute and the Federation of Electric Power Companies of Japan, 2005. *Second progress Report on Research and Development for TRU Waste Disposal in Japan.* JNC and FEPC, Japan, JNC-TY1400-2005-013.

[3] Villar, M. V., 2006. "Infiltration tests on a granite/bentonite mixture: Influence of water salinity," *Applied Clay Science*, **31**: 96-109.

[4] Komine, H., et al., 2010. "Hydraulic Conductivity of Some Bentonite in Artificial Seawater," *Journal of Japan Society of Civil Engineers*, **67**(2): 279-287. [in Japanese]

[5] Atkinson, A. 1985. "The time dependence of pH within a repository for radioactive waste disposal," *United Kingdom Atomic Energy Authority*, AERE-R 11777.

[6] Anderson, A., et al., 1989. "Chemical Composition of Cement Pore Solutions," *Cement and Concrete Research*, **19**: 327-332.

[7] Chigira, M. 1991. “Sealing of Rock Fractures Around HLW Repositories (Part 1) A New Hydrothermal Fracture Flow Apparatus and Its Preliminary Application to Self-sealing by Silica,” *CRIEPI Research Report*, U91031. [in Japanese]

[8] Chigira, M. 1993. “Sealing of Rock Fractures Around HLW Repositories (Part 2)—Silica Precipitation Behavior in Flow Fields,” *CRIEPI Research Report*, U92050. [in Japanese]

[9] Chigira, M. 1996. “Sealing of Rock Fractures around HLW Repositories (Part 3)—Silica Precipitation rate, Colloidal Formation, and Pore Closure,” *CRIEPI Research Report*, U95053. [in Japanese]

[10] Sasagawa, T., et al., 2017. “Effects of Supersaturated Silicic Acid Concentration on Deposition Rate Around Geological Disposal System,” *Journal of NUCLEAR ENGINEERING AND RADIATION SCIENCE*, **3** (4): 041010-1–041010-6.

[11] Sasagawa, T., et al., 2017. “Effects of Temperature on the Deposition Rate of Supersaturated Silicic Acid on Ca-type bentonite,” *Journal of Energy and Power Engineering*, **11**: 559-568.

[12] Matyskiela, W. 1997. “Silica redistribution and hydrologic changes in heated fractured tuff,” *Geology*, **25**(12): 1115-1118.

[13] Martin, L. H. J., et al., 2016. “A natural cement analogue study to understand the long-term behaviour of cements in nuclear waste repositories: Maqarin (Jordan),” *Applied Geochemistry*, **71**: 20-34.

[14] Iler, R. K. 1979. *The Chemistry of Silica–Solubility, Polymerization, Colloid and Surface Properties, and Biochemistry*. John Wiley & Sons, New York.

[15] Ito, M., et al. 1994. “Mineral Composition Analysis of Bentonite,” *Journal of Atomic Energy Society of Japan*, **36**(11): 1055-1058.

[16] Eltantawy, M., and Arnold, P.W. 1973. “Reappraisal of Ethylene Glycol Mono-Ethyl Ethel (EGME) Method for Surface Area Estimations of Clays,” *Journal of Soil Science*, **24**(2): 232-238.

[17] Alexander, G. B., 1953. “The Reaction of Low Molecular Weight Silicic Acids with Molybdic Acid,” *Journal of the American Chemical Society*, **75**: 5655.

[18] Chida, T., et al., 2007. “Deposition rate of polysilicic acid with up to 10^{-3} calcium ions,” *Applied Geochemistry*, **22**(12): 2810-2816.

[19] Takahashi, Y., et al., 1988. “Effect of the Concentration of Sodium Chloride on the Polymerization of Silicic Acid,” *Journal of the Geothermal Research Society of Japan*, **10**(3): 225-235. [in Japanese]

[20] Hashimoto, K., 1989. *Chemical Reaction Engineering*, BAIHUKAN CO., LTD. [in

Japanese]

[21] Lasaga, A. C., 2014. *Kinetic Theory in the Earth Sciences*, Princeton University Press.

[22] Weir, G. J. and White, S. P., 1996. “Surface Deposition from Fluid Flow in a Porous Medium,” *Transport in Porous Media*, **25**: 79-96.